Journal of Inflammation Research

Dovepress
Taylor & Francis Group

Open Access Full Text Article

ORIGINAL RESEARCH

The Effects and Mechanisms of Patchouli Alcohol on Experimental Periodontitis Rats Based on the OPG/RANK/RANKL/P38 MAPK Signaling Pathway

Shuting Zhang[1,*], Feifei Duan[1,*], Tianzhen He[1], Chaoqun Sun[1], Menglu Zhen[1], Enxi Liang[1], Xingduo Liu[1], Yuqiong Dai[1], Ruoting Zhan[2,3], Nianchun Hu[4], Yun Xia[5], Sijun Liu[1]

[1]School of Pharmaceutical Sciences, Guangzhou University of Chinese Medicine, Guangzhou, People's Republic of China; [2]Science and Technology Innovation Center, Guangzhou University of Chinese Medicine, Guangzhou, People's Republic of China; [3]Key Laboratory of Chinese Medicinal Resource From Lingnan, Guangzhou University of Chinese Medicine, Guangzhou, People's Republic of China; [4]Department of Neurology, 921 Hospital of the Joint Logistics Support Force, Changsha, People's Republic of China; [5]Luohu District Traditional Chinese Medicine Hospital, Shenzhen, Guangdong Province, People's Republic of China

*These authors contributed equally to this work

Correspondence: Sijun Liu, School of Pharmaceutical Sciences, Guangzhou University of Chinese Medicine, Waihuan Road, Guangzhou Higher Education Mega Center, No. 232, Guangzhou, Guangdong, 510006, People's Republic of China, Email liusijun@gzucm.edu.cn; Yun Xia, Department of Nephropathy, Department of Nephropathy, Luohu District Traditional Chinese Medicine Hospital, Shenzhen Luohu district, Xiantong road 16, CN 518004, Guangdong, China, Email 1595633489@qq.com

Background: Patchouli has been used for a long time in traditional Chinese medicine to treat inflammatory diseases, and its main active component, patchouli alcohol (PA), also has anti-inflammatory effects. However, the underlying molecular mechanism of PA in the periodontitis treatment is not well understood.

Aim of the Study: The primary objective of this study was to examine the effects of PA on experimental periodontitis in rats through the lens of the OPG/RANK/RANKL/p38 MAPK signaling pathway.

Materials and Methods: A rat model of periodontitis induced by ligation combined with LPS injection was used to evaluate the therapeutic effects of PA on periodontitis. Target prediction, target screening, intersection target identification, protein-protein interaction (PPI) network construction and topological analysis, Gene Ontology (GO) and Kyoto Encyclopedia of Genes and Genomes (KEGG) enrichment analyses, along with molecular docking were employed to predict the potential pharmacological mechanisms of PA. Micro-CT was utilized to detect alveolar bone loss, ELISA was used to measure inflammation, and qRT-PCR and Western blot were performed to further confirm its mechanisms of action.

Results: Network pharmacology indicated that the p38 MAPK signaling pathway is the primary mechanism by which PA treats periodontitis. PA treatment reduced the distance between the cementum and the alveolar bone crest in rats with periodontitis. ELISA and H&E staining results showed that PA alleviated the inflammatory response and reduced the levels of IL-6, TNF-α, and IL-1β. qRT-PCR analysis revealed that PA significantly increased the mRNA expression levels of *RUNX2* and *OPG*, and decreased the mRNA expression levels of *RANK, RANKL, NFATc1*, and *TRAF6*. Western blot revealed that PA significantly reduced the expression of RANKL, RANK, and MMP9 while significantly elevating OPG expression.

Conclusion: PA is an effective therapeutic strategy for periodontitis, and its mechanism of action involves inhibiting alveolar bone loss and modulating the OPG/RANK/RANKL/p38 MAPK pathway.

Keywords: network pharmacology, molecular docking, periodontitis, patchouli alcohol, inflammation, alveolar bone loss

Introduction

Periodontitis is a classic infectious disease among periodontal disorders and is characterized by persistent inflammatory responses in periodontal tissues and progressive damage or destruction of cementum, alveolar bone, and periodontal ligament.[1] Periodontitis contributes to multiple systemic comorbidities, particularly malnutrition-related disorders and

Received: 26 March 2025
Accepted: 27 August 2025
Published: 13 September 2025

Graphical Abstract

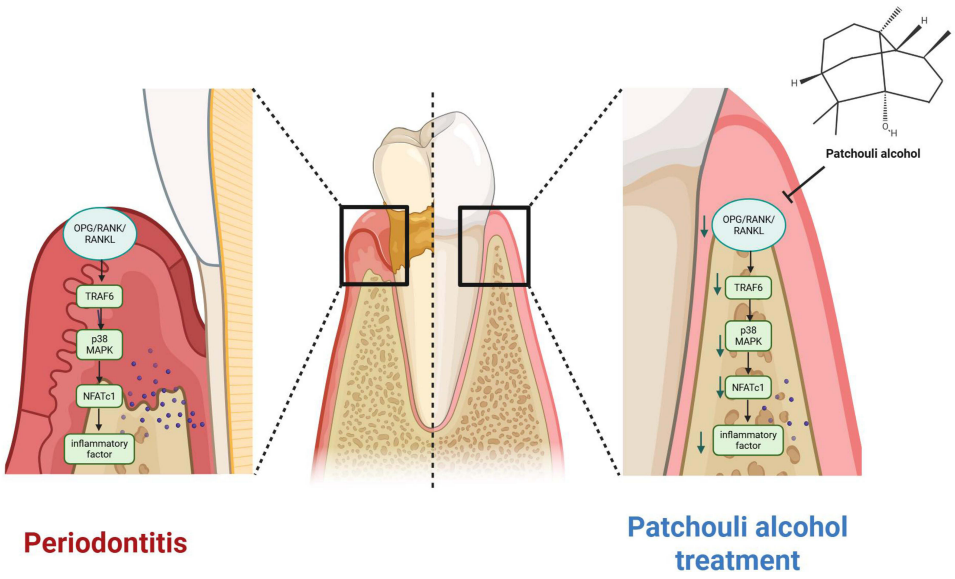

cardiovascular diseases, imposing substantial burdens on healthcare systems.[2,3] Epidemiological evidence indicates that disease progression correlates with age, gender, oral hygiene, and dietary habits.[4] Periodontitis ranks among the most prevalent oral infectious diseases globally, affecting over 700 million people, representing 11% of the world's population.[5] The scaling and root planning, which is a primary treatment strategy, shows limited therapeutic efficacy and often requires adjunctive pharmacological interventions. Additionally, current clinical outcomes of these modalities remain suboptimal.[6] Therefore, identifying and developing novel pharmacotherapeutic agents for periodontitis is urgently needed.

RANKL is recognized as the master differentiation factor for osteoclastogenesis. Hence, osteoprotegerin (OPG)/ the receptor activator of nuclear factor-κB (RANK) / receptor activator of nuclear factor-κB ligand (RANKL) axis constitutes a pivotal regulatory mechanism in bone metabolism research. During alveolar bone remodeling, the OPG/RANKL/RANK signaling pathway participates in osteoclast differentiation and formation, thereby modulating bone resorption.[7] RANKL serves as the principal regulator of osteoclast differentiation, while OPG acts as a decoy receptor for RANKL. OPG binds RANKL with high affinity, preventing the interaction between RANKL and its receptor RANK. The binding of RANK and RANKL activates TRAF6, leading to the phosphorylation of proteins.[8] This subsequently activates MAPKs signaling pathways, including c-Jun N-terminal kinase (JNK), p38, and extracellular signal-regulated kinase (ERK). The activation of these pathways ensures the differentiation of osteoclast precursors, subsequently regulating the expression of activator protein-1 (AP-1), ultimately promoting osteoclastogenesis.[9] Consequently, inhibiting elevated RANKL expression or modulating the RANKL/OPG ratio, coupled with controlling the appropriate infection, may represent an effective strategy for preventing bone destruction in periodontitis.

The application of natural medicines in periodontitis treatment has a long historical lineage. Since ancient times, herbal medicines have been widely employed to treat various ailments, including periodontitis, which is a prevalent oral disease.[10] Approximately 80% of the global population utilizes Chinese herbal medicines for health maintenance and disease prevention. PA, a sesquiterpene compound with the chemical formula $C_{15}H_{26}O$, is primarily extracted from the essential oil of *Pogostemon cablin* (patchouli). Modern pharmacological studies reveal that PA exhibits anti-inflammatory,[11] antibacterial,[12] and neuroprotective properties,[13] effectively suppressing lipopolysaccharide (LPS)-induced inflammation in conditions such as mastitis and acute lung injury (ALI).[14]

Current research indicates that Pogostemon cablin (patchouli) and its extracts can alleviate periodontitis by inhibiting the proliferation of oral microorganisms.[9] Furthermore, patchouli may also mitigate periodontitis-induced bone destruction by modulating the NF-κB-mediated inflammatory pathway. However, whether its active constituent, patchoulol, can directly ameliorate alveolar bone resorption caused by periodontitis through regulation of the OPG/RANK/RANKL pathway remains unclear. However, its role in preventing or treating periodontal diseases remains unclear and warrants further investigation.

This study constructed a target database from traditional Chinese medicine (TCM) repositories and applied network pharmacology and molecular docking to identify the therapeutic targets and mechanisms of patchoulol against periodontitis. A rat periodontitis model was established through silk ligation with local LPS injection. The therapeutic effects of PA on alveolar bone remodeling were assessed using micro-computed tomography (micro-CT). Key osteoclast-related factors and proteins in the p38 mitogen-activated protein kinase (MAPK) pathway were quantified via Western blot (WB) and quantitative polymerase chain reaction (qPCR). Secretion levels of pro-inflammatory cytokines in periodontal tissues were determined by enzyme-linked immunosorbent assay (ELISA). This research aims to validate PA's efficacy in periodontitis treatment and elucidate its molecular mechanisms, providing scientific evidence for TCM-based clinical interventions in periodontitis-related disorders.

Materials and Methods

PA Structure Acquisition and Target Prediction

The Traditional Chinese Medicine Systematic Pharmacology Database and Analysis Platform (TCMSP, http://tcmspw.com/tcmsp.php) is a free and continuously updated important database of Chinese medicinal resources, which includes chemical and pharmacological information related to PA. The TCMSP database retrieves the chemical structure of PA and related biological targets. By searching the PubChem database (https://pubchem.ncbi.nlm.nih.gov/), the chemical structure of PA is exported as an "SDF" file, and the data of the "SDF" file is input into the Swiss Target Prediction database (http://swisstargetprediction.ch/) to obtain predicted targets for PA. At the same time, the chemical structure of PA is imported into the PharmMapper database (https://lilab-ecust.cn/pharmmapper/index.html), and the reverse docking principle is used to obtain predicted targets for PA. The target points of PA obtained from the above three databases are merged and imported into the UniProt database (https://www.uniprot.org/), and potential pharmacological targets of PA are analyzed and annotated. The candidate targets are all modified to official standardized abbreviations, namely Gene symbols, and duplicate targets as well as non-human and non-standard targets are removed.

Screening of Targets Related to Periodontitis

With periodontitis as the keyword, search for potential targets of periodontitis in the DrugBank database (https://go.drugbank.com/), GeneCards database (https://www.genecards.org/), the "GeneMap" of OMIM database (https://www.omim.org/), and the "disease" section of DisGeNET database (https://disgenet.com/). Integrate the periodontitis gene targets retrieved from the four databases and remove duplicate values to obtain relevant target genes for periodontitis.

Screening the Intersection Targets of PA and Periodontal Diseases

The periodontal disease-related targets were imported into the UniProt database for analysis and validation. Duplicate entries were removed, and their corresponding protein names and standardized gene symbols were retrieved. Finally, the Venn diagram analysis function in R software (version 4.1.2) was utilized to identify overlapping targets between periodontal disease and PA. These common targets were selected as the potential therapeutic targets through which PA may prevent or treat periodontal disease.

Protein-Protein Interaction (PPI) Network Construction and Topological Analysis

The potential target set of PA for periodontitis was imported into the STRING database. The species was specified as "Homo sapiens", and the PPI network was constructed with a minimum interaction score threshold set to >0.4.

Gene Ontology (GO) and Kyoto Encyclopedia of Genes and Genomes (KEGG) Enrichment Analysis

The Metascape database was utilized to perform Gene Ontology (GO) functional analysis on the potential targets of patchoulol for periodontitis treatment. The GO system comprises three ontology categories: Molecular Function (MF), Cellular Component (CC), and Biological Process (BP), which describe the specific functions of gene products, their cellular localization, and associated biological processes, respectively. Subsequently, the target genes related to periodontitis prevention and treatment were uploaded to the Metascape platform for KEGG pathway analysis. During the analysis, a significance threshold of $p < 0.01$ was applied as the screening criterion. The resulting data were imported into the microbial bioinformatics platform for visualization.

Molecular Docking

Export the PA mol2 format from TCMSP and open it with PyMOL 2.5.5 software, saving it as a PDB file. Use AutoDock 1.5.7 to hydrogenate it, setting PA as the ligand and exporting it as a PDBQT format ligand file. Obtain the 3D structure of the core protein from the PDB database and preprocess it with PyMOL. AutoDock Vina 1.1.2 was used to dock PA and the core protein.

Animal Treatment

Forty male Sprague-Dawley (SD) rats of specific pathogen-free (SPF) grade, weighing 180–220 g, were provided by Rigel Animal Company (Approval No.: SYXK (Yue) 2024–0202). The animals were housed under standardized conditions: 12-hour light/dark cycle, temperature controlled at 22 ± 2°C, humidity maintained at ~60%, and ad libitum access to food and water. Following a 7-day acclimatization period, all experimental procedures were conducted in strict accordance with the guidelines of the Chinese Committee on the Use of Laboratory Animals and the principles for animal care and use, as approved by the Ethics Committee of Guangzhou University of Chinese Medicine.

Drug Preparation

PA was dissolved in physiological saline containing 2% (v/v) DMSO and 1% (v/v) Tween 80, followed by sonication in a water bath to prepare solutions at 4 mg/mL and 2 mg/mL. Separately, minocycline hydrochloride was dissolved in physiological saline to prepare a homogeneous solution.

Grouping and Dosing of Experimental Animals

Rats were anesthetized via intraperitoneal injection of pentobarbital sodium (1 mg/100 g body weight) prepared as a 0.3% (w/v) solution. Upon observing decreased respiratory rates and complete muscle relaxation, animals were fixed in a supine position on the surgical table. Using fine-tipped forceps, a 0.2 mm sterile orthodontic ligature wire was looped around the cervical regions of the right maxillary first and second molars. The wire was embedded into the gingival sulcus, knotted, and trimmed to remove excess ends. Postoperatively, daily LPS injections were administered for 14 days to establish a validated periodontitis model. Modeled rats were randomly allocated into five groups ($n = 8$): a control group (Control) and model group (Model) receiving an equivalent volume of normal saline via oral gavage, a positive control group administered minocycline hydrochloride (MH, 64.8 mg/kg/day); two PA-treated groups receiving 20 mg/kg/day (PA (20 mg/kg)) and 40 mg/kg/day (PA (40 mg/kg)), respectively. All treatments were maintained for 4 weeks. Minocycline hydrochloride tablets were pulverized into a fine powder, homogenized in distilled water to form a suspension, and vortex-mixed prior to administration.

Micro-Computed Tomography (Micro-CT) Analysis

Micro-CT scanning was performed using the following parameters: X-ray source voltage 90 kV, current 88 μA, scan duration 4 minutes, field of view (FOV) 18 mm, high-resolution mode, and pixel size 36.00 μm. The distance between the cementoenamel junction (CEJ) and alveolar bone crest (ABC) was measured as the CEJ-ABC distance. Three regions per sample were measured, and the mean value of these distances was calculated for each rat (Figure 1A). Following

region of interest (ROI) selection, alveolar bone microstructure parameters were analyzed. ROI selection was standardized based on anatomical landmarks and predefined dimensions, as described previously[15] (Figure 1B). Quantitative measurements were conducted using image analysis software.

Histological Analysis

The left maxillary alveolar bones of experimental rats were fixed in 4% paraformaldehyde (PFA) for 24 hours and decalcified in 0.5 M ethylenediaminetetraacetic acid (EDTA, pH 7.4) for 14 days. Following paraffin embedding, mesiodistal sections (5 μm thickness) through the first molar and adjacent gingival and alveolar bone tissues were prepared. Tissue sections were stained with hematoxylin and eosin (H&E; Sevile Biotechnology, China) and Masson's trichrome staining (G1006, Servicebio, Wuhan, China) according to the manufacturers' protocols. Stained sections were analyzed using a light microscope at ×400 magnification for histomorphometric evaluation.

Histopathological scoring criteria were evaluated as follows in Table 1.[16]

Western Blotting

Proteins were extracted from maxillary bone tissues using a commercial kit (KGP 250, KeyGEN BioTECH, Nanjing, China). Protein concentrations were quantified via a Bradford assay (KGA 801, KeyGEN BioTECH). Proteins were separated by SDS-PAGE (12% gel) and transferred onto polyvinylidene difluoride (PVDF) membranes (Millipore, Darmstadt, Germany). Membranes were blocked with 5% bovine serum albumin (BSA) for 1 h at room temperature, followed by overnight incubation at 4 °C with the following primary antibodies: anti-OPG (R1608-4, HUABIO, 1:1000), anti-RANK (ER1915-70, HUABIO, 1:2000), p38 MAPK (2286T, CST, 1:1000), phospho-p38 MAPK (4511T, CST, 1:1000), RANKL (23408-1-AP, Proteintech, 1:1000), β-actin (GB111557-50, servicebio, 1:10000) and GAPDH (ET1601-4, HUABIO, 1:160,000). After washing, membranes were incubated with HRP-conjugated secondary antibodies (1:5000) for 1 h at 25 °C. Protein bands were visualized using enhanced chemiluminescence (36223ES60, YEASEN, Shanghai, China) and quantified via ImageJ software.

Quantitative Real-Time PCR (qRT-PCR) Assay

Gene transcription levels associated with periodontitis progression in gingival tissues were analyzed by quantitative reverse transcription PCR (qRT-PCR), following established protocols. Total RNA was extracted from tissues using TRIzol™ Reagent (T9424, Sigma-Aldrich, USA). RNA concentration and purity were assessed with a NanoDrop 2000 spectrophotometer (Thermo Fisher Scientific, USA). First-strand cDNA was synthesized from 1 μg RNA using a High-Capacity cDNA Reverse Transcription Kit (Thermo Fisher Scientific). qRT-PCR amplification was performed on a CFX96 Touch™ system (Bio-Rad, USA) under the following conditions: initial denaturation at 95°C for 30s, followed by 40 cycles of denaturation (95°C, 10s) and annealing/extension (60°C, 30s). Relative gene expression was calculated via the $2^{-\Delta\Delta Ct}$ method using threshold cycle (Ct) values. Primer sequences are provided in Table 2.

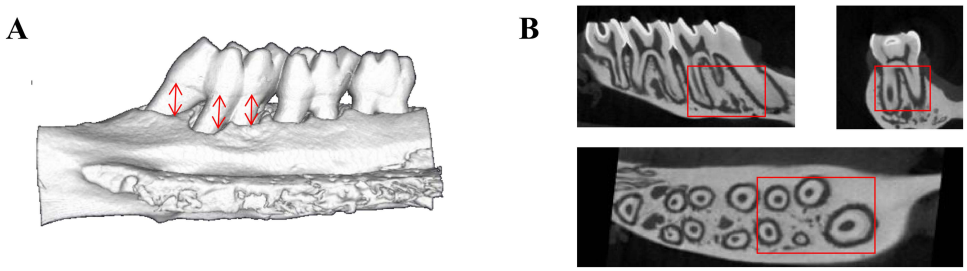

Figure 1 (**A**) Arrows show the buccal distance from CEJ to ABC as a marker of alveolar bone height; the length of CEJ-ABC was measured at three locations (mesial, central, and distal) of maxillary M1, and the average value was taken as Experimental data. (**B**) Select a cuboid region as ROI to evaluate the microstructural parameters of alveolar bone.

Table 1 Histopathological Scoring Criteria Were Evaluated

Grade	Inflammatory Infiltration	Alveolar Process	Cementum Structure
0	Absent or minimal scattered inflammatory cell infiltration	Intact	Intact
1	Moderate inflammatory cell infiltration	Mild resorption	Intact
2	Substantially increased inflammatory cell infiltration	Exacerbated resorption	Partial destruction, structural continuity remained retained without complete disruption.
3	Severe inflammatory cell infiltration	Complete resorption	Extensive destruction

Table 2 Primes for qRT-PCR

Gene	Forward (5'-3')	Reverse (5'-3')
β-actin	AGGAGAAGCTGTGCTACGTC	AATGCCAGGGTACATGGTGG
IL-1β	TGCCACCTTTTGACAGTGATG	GGAGCCTGTAGTGCAGTTGT
MMP-9	ACCTCCAACCTCACGGACA	AGGTTTGGAATCGACCCACG
RANKL	CCTGTACTTTCGAGCGCAGA	GCATTGATGGTGAGGTGTGC
RANK	AGCAGATGCGAACCAGGAAA	CCTTGTTGAGCTGCAAGGGA
OPG	GTCATGATTGCCTGGGCTGC	TGTTCATTGTGGTCCTCGGG
RUNX2	CACAGTGGTAGGCAGTCCCA	GGAGAAAGTTTGCACCGCAC

Enzyme-Linked Immunosorbent Assay (ELISA)

According to the manufacturer's instructions, use a multifunctional microplate reader to measure the levels of IL-6, TNF-α and IL-1β using a detection reagent kit (Meimian, Jiangsu, China).

Statistical Analysis

Statistical analyses were performed using SPSS 26.0 (IBM, USA). Continuous variables are presented as mean ± standard deviation (SD) if normally distributed (Shapiro–Wilk test, $p > 0.05$). For intergroup comparisons of parametric data, one-way analysis of variance (ANOVA) was applied. When homogeneity of variance was confirmed (Levene's test, $p > 0.05$), post hoc comparisons were conducted using the least significant difference (LSD) test; otherwise, Dunnett's T3 test was employed. Non-normally distributed data ($p < 0.05$) were analyzed by the Kruskal–Wallis *H*-test, with the Mann–Whitney *U*-test for pairwise comparisons. A significance level of $p < 0.05$ was applied. Graphical presentations were generated using GraphPad Prism 8.0 (GraphPad Software, USA).

Results

PA and Periodontitis Intersection Target Screening

The chemical structure of PA is shown in Figure 2A. In the GeneCards database, 3239 periodontal disease gene targets were obtained, and 1421 targets with scores greater than 1 were screened out for further analysis. Genetic targets for periodontal disease were retrieved from the OMIM database. After merging and de-duplicating, 14 periodontal disease gene targets were obtained. In the DisGeNET database, 683 periodontal disease gene targets were identified. In the DrugBank database, 11 periodontal disease gene targets were retrieved. The periodontal disease gene targets retrieved from the four databases were organized and de-duplicated, resulting in a total of 1716 periodontal disease gene targets (Figure 2B).

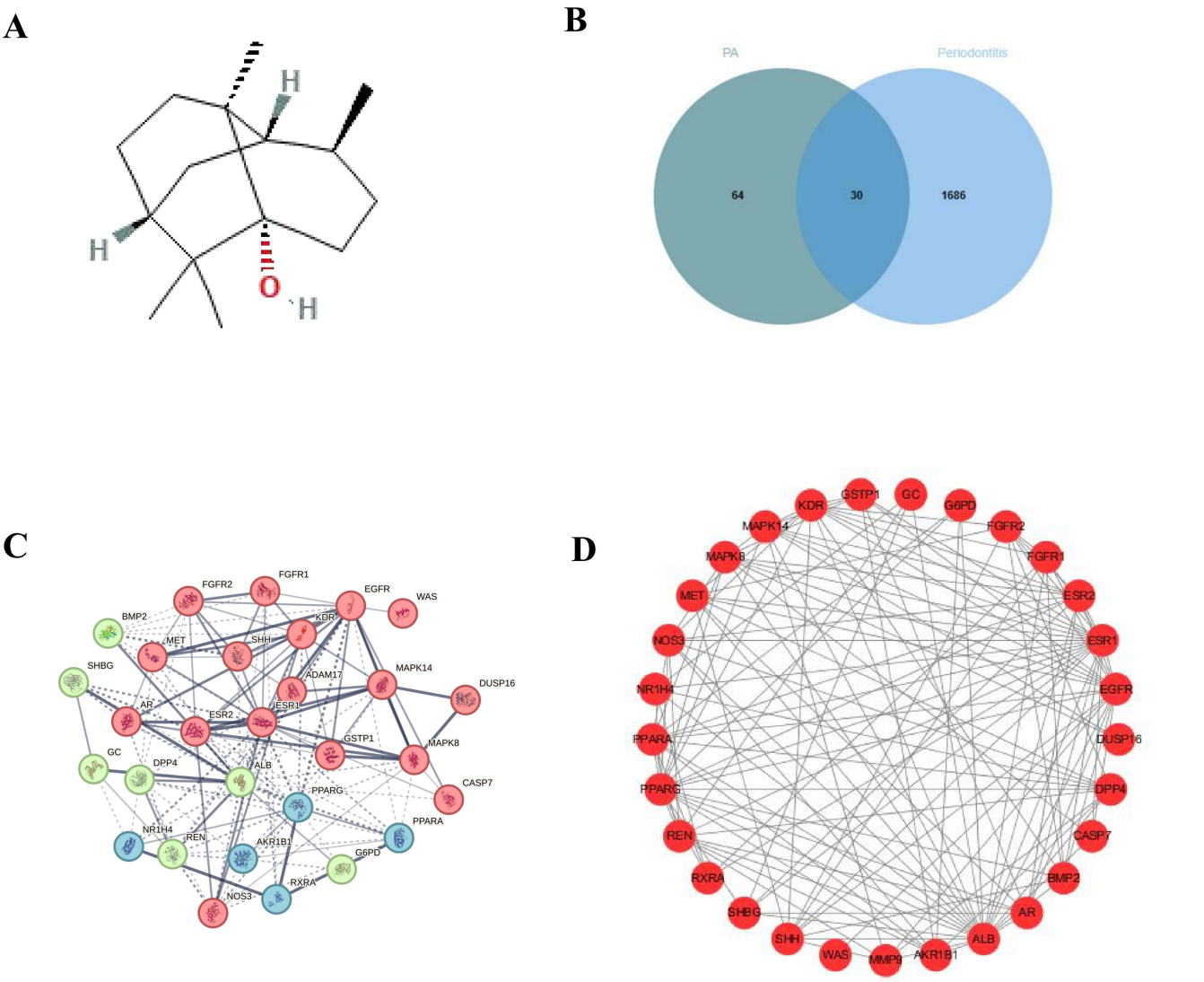

Figure 2 (**A**) The chemical structure of PA (**B**) Venn diagram of PA and periodontitis (**C**) Cross-PPI networks (**D**) PPI network core screening.

PPI Network Analysis and Core Target Selection

To construct a PPI network of 30 intersecting targets using the STRING database, there are a total of 30 nodes and 136 edges. The average degree of the nodes is 9.07. The interaction relationships between proteins are represented by each edge, and each node represents each target protein (Figure 2C and D).

GO Enrichment Analysis

A total of 560 Gene Ontology (GO) entries ($p < 0.01$) were identified, comprising 496 biological process (BP), 48 molecular function (MF), and 16 cellular component (CC) terms. The top 10 significantly enriched GO-BP, GO-MF, and GO-CC entries are visualized in Figure 3A. BP analysis revealed processes including cellular response to lipids, regulation of hormone levels, branching epithelium morphogenesis, positive regulation of phosphorus metabolism, hormone-mediated signaling, mesenchymal cell proliferation, steroid metabolism, rhythmic processes, regulation of muscle cell differentiation, and nutrient response. MF terms encompassed nuclear receptor activity, transmembrane receptor tyrosine kinase activity, monocarboxylic acid binding, mitogen-activated protein (MAP) kinase activity, protein domain-specific binding, endopeptidase activity, exogenous protein binding, hormone

https://doi.org/10.2147/JIR.S530534

binding, actin binding, and glycosaminoglycan binding. CC annotations included membrane rafts, leading edge membranes, cell projection membranes, and apical plasma membranes.

KEGG Pathway Enrichment Analysis

KEGG enrichment analysis revealed significant enrichment ($p < 0.01$) in 86 signaling pathways. Figure 3B displays the top 20 of the most statistically significant pathways using a bubble plot. Major pathway clusters included oncogenic pathways (eg, Pathways in cancer, PI3K-AKT signaling), infection response (eg, Epithelial cell signaling in Helicobacter pylori infection), and metabolic regulation (eg, Non-alcoholic fatty liver disease).

Molecular Docking Analysis of PAs with Intersection Targets

Molecular docking simulations were performed using AutoDock Vina to (a) predict the spatial compatibility of PA with the binding pockets of target proteins, and (b) calculate ligand-receptor binding affinities. The calculated binding energy (ΔG), a key evaluation metric, indicates spontaneous molecular interactions when values are below 0 kcal/mol. Thermodynamic analysis revealed an inverse correlation between ΔG values and binding stability, and lower energy states indicate stronger ligand-receptor affinity and higher interaction probability. Quantitative binding energy data for PA with key therapeutic targets are summarized in Table 3.

Effects of the PA on Alveolar Bone Loss in Maxillae of Lipopolysaccharide-Induced Rats

Micro-CT analysis was conducted across all experimental groups (Figure 4A). Measurements of the cementoenamel junction to alveolar bone crest (CEJ-ABC) distance were performed at mesial, central, and distal sites of the first molar (M1). The results showed that after 4 weeks of administration, the CEJ-ABC distance in the Model was significantly greater than that in the Control, MH, PA (20 mg/kg), and PA (40 mg/kg), with statistically significant differences ($p < 0.05$). Additionally, the CEJ-ABC distance in the PA (40 mg/kg) was closer to that in the Control (Figure 4B). Regarding the BV/TV (%), compared with the Control, the BV/TV value in the Model was significantly reduced ($p < 0.05$), indicating a notable decrease in bone volume within the alveolar bone. However, the BV/TV values in the drug intervention groups (MH, PA (20 mg/kg), and PA (40 mg/kg)) were significantly higher than that in the Model, suggesting that the drug intervention effectively increased bone volume (Figure 4C). In addition, compared with the Control, the trabecular thickness (Tb.Th) in the Model was significantly reduced ($p < 0.001$), indicating thinning of the trabecular structure. The trabecular thickness in the MH, PA (20 mg/kg), and PA (40 mg/kg) was higher than that in the Model, and the Tb.Th in the PA (40 mg/kg) was close to that in the Control, suggesting that high-dose drug intervention effectively restored trabecular thickness (Figure 4D). As for the Trabecular Separation (Tb.Sp) result, compared with the Control, the trabecular separation in the Model was significantly increased ($p < 0.001$), indicating enlarged trabecular spaces and osteoporotic bone structure. Compared with the Model, the drug intervention groups, including MH, PA (20 mg/kg), and PA (40 mg/kg), exhibited lower values in trabecular separation. Furthermore, the trabecular spaces in the PA (40 mg/kg) were similar to those in the Control, demonstrating that this drug intervention effectively reduced trabecular separation, thereby restoring bone structure (Figure 4E). These quantitative analyses demonstrate PA's potential in ameliorating alveolar bone loss and trabecular microstructure deterioration.

Effects of the PA on the Histopathology of Periodontitis

H&E staining results revealed that the first molar interdental region of experimental animals in the Model exhibited typical inflammatory pathological changes in periodontal tissues, which were consistent with the imaging features obtained from Micro-CT scans. Specific manifestations included gingival papilla recession below the cementoenamel junction (CEJ), reduction in alveolar bone crest height, and the formation of pathological periodontal pockets. Additionally, the connective tissue structure was disorganized, with partial degeneration of periodontal ligament fibers and detachment from the root surface, no longer tightly attached to the cementum. Significant infiltration of inflammatory cells, primarily neutrophils, and lymphocytes were observed in the gingival tissue, while bone resorption lacunae were

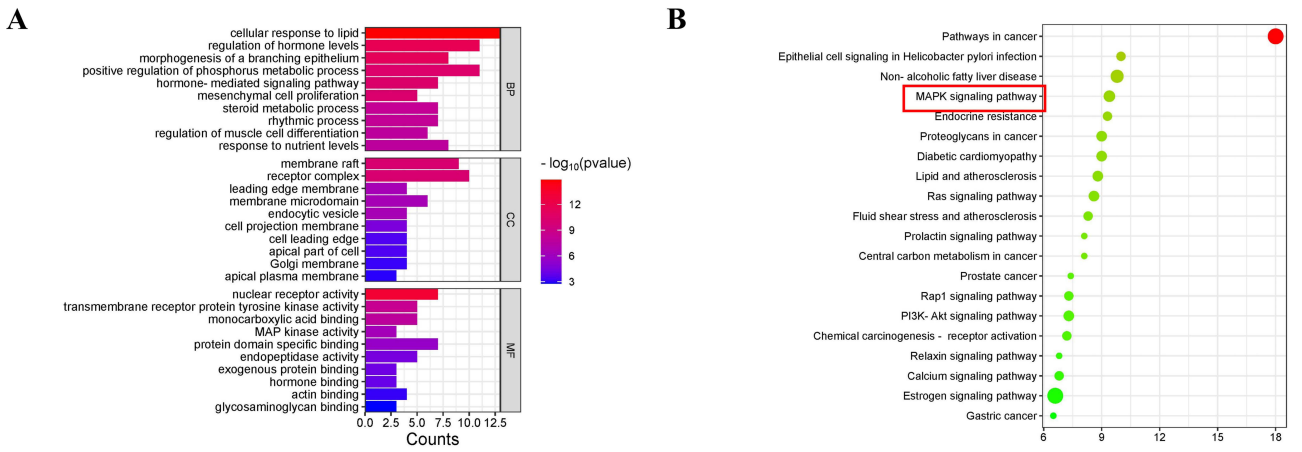

Figure 3 GO and KEGG enrichment analysis on anti-periodontitis mechanisms of PA. (**A**) The top 10 significantly enriched (p <0.05) terms in BP, CC and MF of GO analysis (**B**) KEGG enrichment analysis on anti-periodontitis mechanisms of PA. The top 20 pathways with significantly enriched (P<0.05).

detected in the alveolar crest region. In contrast, rats in the PA (20 mg/kg) and PA (40 mg/kg) showed moderate or mild inflammatory cell infiltration in periodontal tissues after drug intervention, with relatively intact alveolar bone structure (Figure 5A). Further analysis of inflammatory scores in periodontal tissues across experimental groups indicated that the

Table 3 Binding Abilities Between PA and Target Proteins

Gene Name	Binding Afnity
ADAM17	−5.9
AKR1B1	−5.6
ALB	−8.9
AR	−6.8
BMP2	−6.3
DPP4	−8.1
EGFR	−6.2
ESR1	−8.0
FGFR1	−7.7
FGFR2	−6.1
G6PD	−6.0
GABBR1	−6.8
GSTP1	−6.4
KDR	−6.0
MAPK8	−6.4
MAPK10	−6.0
MAPK14	−7.7
MET	−6.9
NOS3	−6.8
NR1H4	−6.2
PPARA	−7.7
PPARG	−6.5
REN	−7.7
RXRA	−7.4
SHBG	−8.7
SHH	−6.2
WAS	−5.8

https://doi.org/10.2147/JIR.S530534

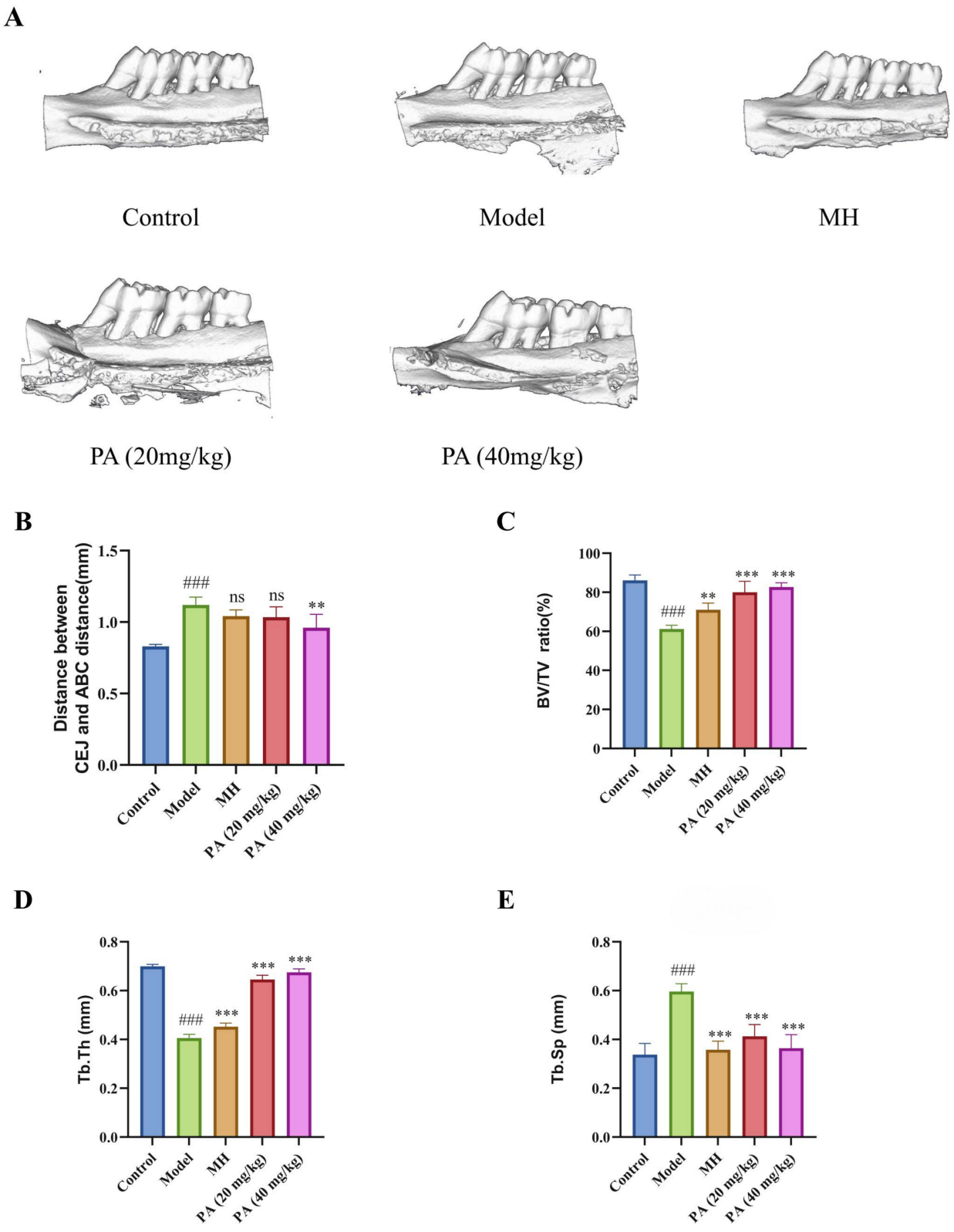

Figure 4 (**A**) Micro-CT images. (**B**) Representative reconstruction of micro-CT of the maxilla. On the sagittal side, radiographic bone loss was measured from cementoenamel junction (CEJ) to alveolar bone crest (ABC) for the maxillary first molar; (**C**) BV/TV (%); (**D**) Tb.Th; (**E**) Tb.Sp; Data is expressed as mean ± standard deviation (n=4). Compared with the Control, $^{###}p < 0.001$; compared with the Model, $^{**}p < 0.01$, $^{***}p < 0.001$; *ns*=not significant ($p > 0.05$).

PA (40 mg/kg) exhibited significantly reduced alveolar bone loss and periodontal inflammation compared to the Model ($p < 0.05$), suggesting that this dosage had the optimal anti-inflammatory effect (Figure 5B).

Histopathological observations using Masson staining revealed that in the Model samples, the number of collagen fibers in the gingival tissue was reduced, with sparse collagen arrangement and decreased adhesion. In the drug intervention groups (MH, PA (20 mg/kg), and PA (40 mg/kg)), collagen fiber bundles exhibited varying degrees of aggregation, with the PA (40 mg/kg) showing significant remodeling effects (Figure 6).

Analysis of Periodontal Tissues of Second Maxillary Molars

The mRNA expression levels of *RUNX2* and *OPG* in the Model were significantly lower than those in the Control ($p < 0.05$). However, after treatment with PA, the mRNA expression levels of *RUNX2* and *OPG* significantly increased ($p < 0.05$), indicating that PA promotes osteogenesis in rat alveolar bone (Figure 7A and B). Compared with the Control, the mRNA levels of *RANK* and *RANKL* in the Model were significantly elevated ($p < 0.05$). After treatment with PA, the mRNA levels of *RANK* and *RANKL* significantly decreased ($p < 0.05$), suggesting that PA significantly reduces the expression of osteoclast-related factors in rat alveolar bone (Figure 7C and D). Compared with the Control, the mRNA levels of *NFATc1* and *TRAF6* in the Model were significantly higher ($p < 0.05$). After treatment with PA, the mRNA levels of *NFATc1* and *TRAF6* significantly decreased ($p < 0.05$), indicating that PA improves periodontitis by inhibiting the p38 MAPK signaling pathway (Figure 7E and F).

Western blot results showed that compared with the Control, the levels of RANKL, RANK, and MMP9 in the Model were significantly increased ($p < 0.001$), while the level of OPG was significantly decreased ($p < 0.001$). After drug intervention, the expressions of RANKL, RANK, and MMP9 were significantly reduced ($p < 0.05$) while the expression of OPG was significantly increased ($p < 0.05$) (Figure 8A-D). These results confirmed that PA significantly reduces the expression of osteoclast-related factors and promotes osteogenic activity in rat alveolar bone in a dose-dependent manner. Compared with the Control, the p-P38 MAPK/p38 MAPK ratio in the periodontal tissues of the Model was significantly increased ($p < 0.001$). After treatment with PA and minocycline hydrochloride, the expression of p-P38 MAPK/p38 MAPK was downregulated ($p < 0.05$) (Figure 8E).

PA Reduces Inflammatory Factors

Compared with the Control, the expressions of inflammatory factors IL-6, TNF-α and IL-1β in the Model were significantly increased ($p < 0.001$). In contrast, the expressions of IL-6, TNF-α and IL-1β in the drug intervention groups (MH, PA (20 mg/kg), and PA (40 mg/kg)) were significantly reduced compared to the Model (Figure 9A–C).

Discussion

Periodontitis is a chronic infectious disease affecting the periodontal supporting tissues, characterized by a progressive pathological process.[17] The primary pathological changes include persistent inflammatory responses in gingival connective tissues, accompanied by alveolar bone resorption, dissociation of periodontal ligament structures, and irreversible damage to the mineralized tissues on the root surface. According to the World Health Organization (WHO), the global prevalence of periodontitis ranges from 20% to 50%, with severe cases accounting for approximately 10%–15%. Data from 2019 revealed that around 1.1 billion people worldwide suffered from periodontitis, including roughly 91.5 million incident cases.[18] Periodontitis triggers chronic inflammation that not only causes progressive alveolar bone resorption but also establishes a vicious cycle with systemic inflammatory responses, contributing to therapeutic challenges.[1] In this study, a periodontitis model was successfully established within two weeks using orthodontic wire ligation combined with LPS injection. In clinical treatment, antibacterial and anti-inflammatory therapies are commonly used for periodontitis. Minocycline hydrochloride, which treats periodontitis through its antibacterial properties, inhibition of collagenase activity, promotion of tissue regeneration, and anti-inflammatory effects, was therefore selected as the positive control drug in this study. Animal models are of great significance in periodontitis research, and this study chose male Sprague-Dawley (SD) rats as experimental animals due to their cost-effectiveness, convenience, simplicity, and well-defined biological characteristics.

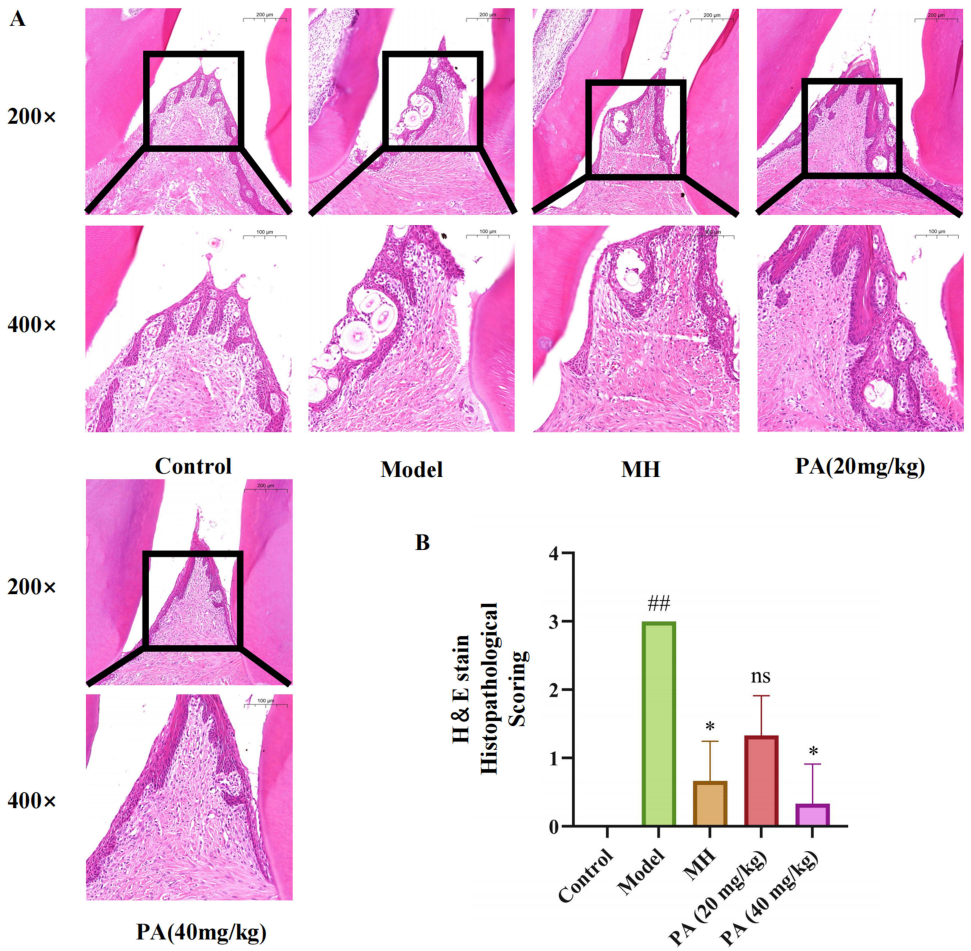

Figure 5 Hematoxylin and eosin (H&E) staining and inflammation scoring (n=3). (**A**) H&E stained histological images of periodontal tissues. (**B**) Statistical Analysis of Histopathological Scores. Magnification: ×200 and ×400. Scale bars: 200 μm and 100 μm.Compared with the Control, $^{\#\#}p < 0.01$; compared with the Model, $^{*}p < 0.05$.

Our network pharmacology investigation revealed that PA's therapeutic effect against periodontitis is largely achieved by modulating the MAPK signaling cascade. Protein–protein interaction analysis identified several core targets of PA, including mitogen-activated protein kinase 8 (MAPK8, also known as JNK1) and MAPK14 (p38), alongside albumin (ALB), estrogen receptor 1 (ESR1), epidermal growth factor receptor (EGFR), and peroxisome proliferator-activated receptor-γ (PPARγ). Notably, the prominence of MAPK8 and MAPK14 among these targets points to the MAPK pathway as a central hub of PA's action, aligning with the known importance of these kinases in periodontal inflammation and alveolar bone remodeling. Consistently, molecular docking simulations showed that PA binds strongly to MAPK10 (JNK3), reinforcing the notion that PA directly targets MAPK signaling components.[19] This direct interaction highlights PA as a promising bioactive compound for the prevention and treatment of periodontitis. Functional enrichment analyses further corroborated these findings. Gene Ontology analysis indicated that PA treatment modulates immune and inflammatory response pathways, consistent with an attenuation of periodontal tissue inflammation. Likewise, KEGG pathway analysis highlighted the MAPK signaling pathway as a key mediator of PA's therapeutic effects, which is notable given that MAPK cascades govern the dynamic balance between alveolar bone destruction and repair. Excessive activation of MAPK pathways is known to tip this balance toward bone loss in periodontitis. Sustained MAPK signaling promotes osteoclastogenesis by upregulating osteoclast-promoting factors such as MMP-9, RANK, and RANKL while downregulating the osteoclast inhibitor OPG, thereby accelerating alveolar bone resorption. At the same time, over-activation of MAPK cascades can impair osteoblast function and new bone formation, compounding the net bone loss. Among the MAPK family members, p38 MAPK emerges as a particularly critical driver of inflammatory bone loss.

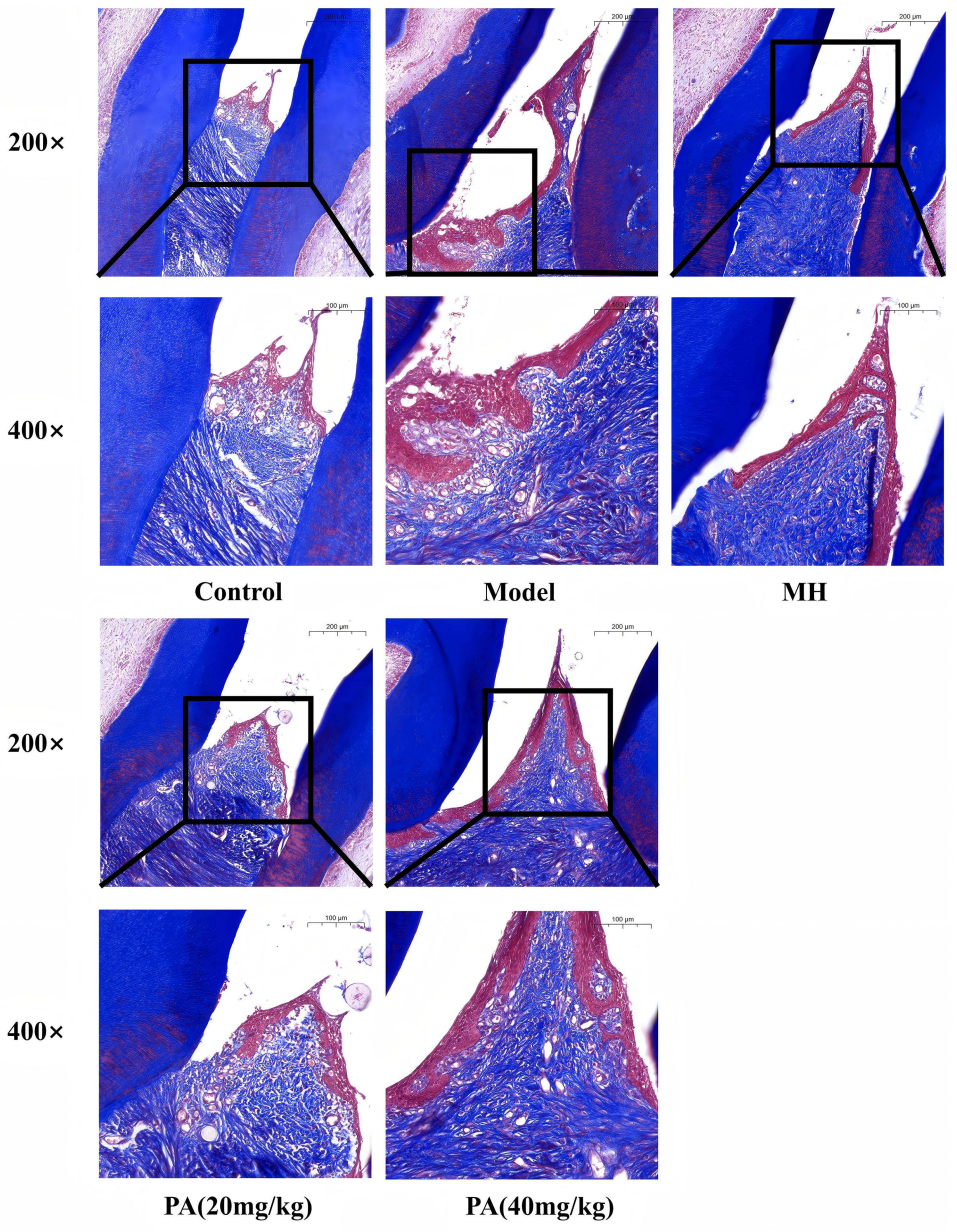

Figure 6 Masson dyeing Magnification: ×200 and ×400. Scale bars: 200 μm and 100 μm.(n=3).

Activation of p38 triggers robust production of pro-inflammatory cytokines and elevates RANKL signaling in osteoclast precursors, driving their differentiation and activity and thus exacerbating bone resorption. For example, the immune regulator Tim4 has been shown to control the phenotype of $CD301b^{+}$ macrophages via the p38 MAPK pathway,[20] illustrating how this signaling axis links the immune response to bone loss in periodontitis. Conversely, blocking the p38 pathway suppresses inflammatory cytokine release and reduces osteoclast formation, mitigating bone resorption—effects observed in periodontitis models and even in systemic bone-loss conditions like osteoporosis. Taken together, these results suggest that PA protects against periodontal bone destruction by interrupting MAPK-driven inflammatory signaling. By inhibiting the overactivation of the p38 MAPK cascade (and potentially other stress-activated MAPK branches such as JNK), PA may break the vicious cycle of inflammation and oxidative stress that underlies periodontal tissue damage. We propose that PA mitigates LPS-induced alveolar bone loss by restraining p38 MAPK activation, thereby reducing downstream pro-inflammatory mediators and osteoclastogenic signals. This mechanism underscores the

https://doi.org/10.2147/JIR.S530534

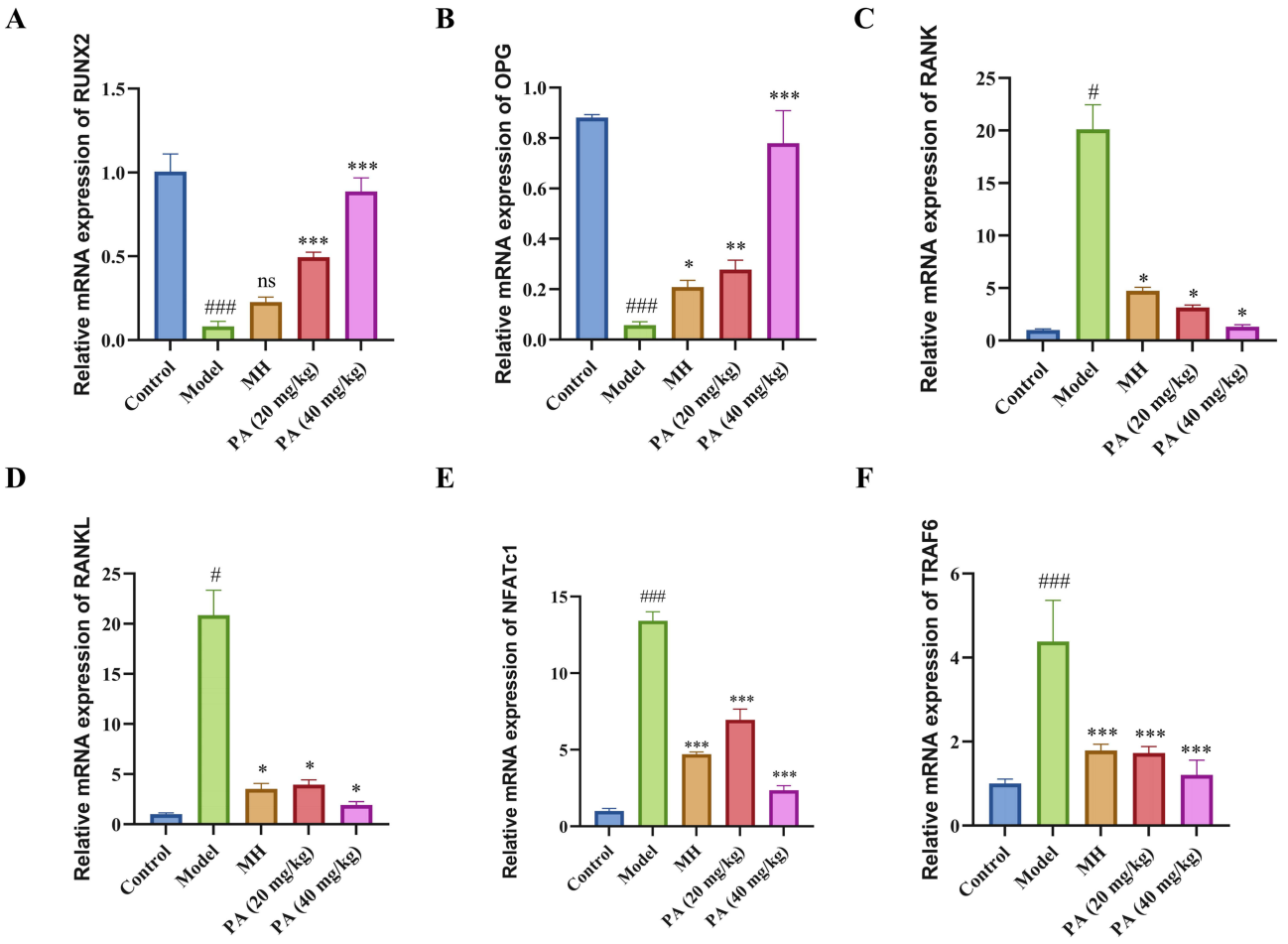

Figure 7 The mRNA expression levels of *RUNX2, OPG, RANK, RANKL, NFATc1* and *TRAF6* in periodontal tissues of rats with periodontitis model by qRT-PCR. (**A**) *RUNX2*; (**B**) *OPG*; (**C**) *RANK*; (**D**) *RANKL*. (**E**) *NFATc1*; (**F**) *TRAF6*. Compared with the Control, $^{\#}p < 0.05$, $^{\#\#\#}p < 0.001$; compared with the Model, $^{*}p < 0.05$, $^{**}p < 0.01$, $^{***}p < 0.001$; *ns*=not significant ($p > 0.05$).

therapeutic potential of PA as a multi-target agent for periodontitis and highlights the value of network pharmacology in identifying critical pathways at the intersection of oxidative stress and periodontal inflammation.

The imbalance of host immune homeostasis is a central regulatory mechanism in the pathological progression of periodontal inflammatory damage. Key pro-inflammatory factors and chemokines in the immune system, including IL-1β, IL-6, and TNF-α, play a pivotal regulatory role in this process. IL-1β holds significant research value in the field of bone metabolism regulation, as it significantly accelerates alveolar bone resorption by activating osteoclast differentiation signaling pathways. IL-6, a pleiotropic cytokine, not only participates in the development of chronic inflammatory diseases but also plays a crucial role in maintaining bone metabolic homeostasis.[21,22] In periodontitis, the IL-6 over-expression can lead to the destruction of periodontal tissues, making it a key biomarker for periodontal tissue detection. Additionally, TNF-α exhibits early activation characteristics in the pathological processes mediated by periodontal microorganisms. Studies have confirmed that this factor promotes disease progression through multiple mechanisms, including enhancing host susceptibility to pathogenic microorganisms, disrupting immune homeostasis, and activating osteoclast function.[23,24] These inflammatory mediators synergistically recruit numerous immune cells and promote tissue degradation by upregulating matrix metalloproteinase (MMP) expression. Among these enzymes, MMP-9 demonstrates a unique dual destructive mechanism, which directly degrades collagen matrices while also promoting osteoclast precursor differentiation through signal transduction pathways.[25] Clinicopathological analyses indicate that MMP-9 concentrations in gingival crevicular fluid and serum show significant positive correlations with clinical inflammation indices in periodontitis patients,[26] particularly demonstrating elevated activity in periapical lesions.[27] Notably, the

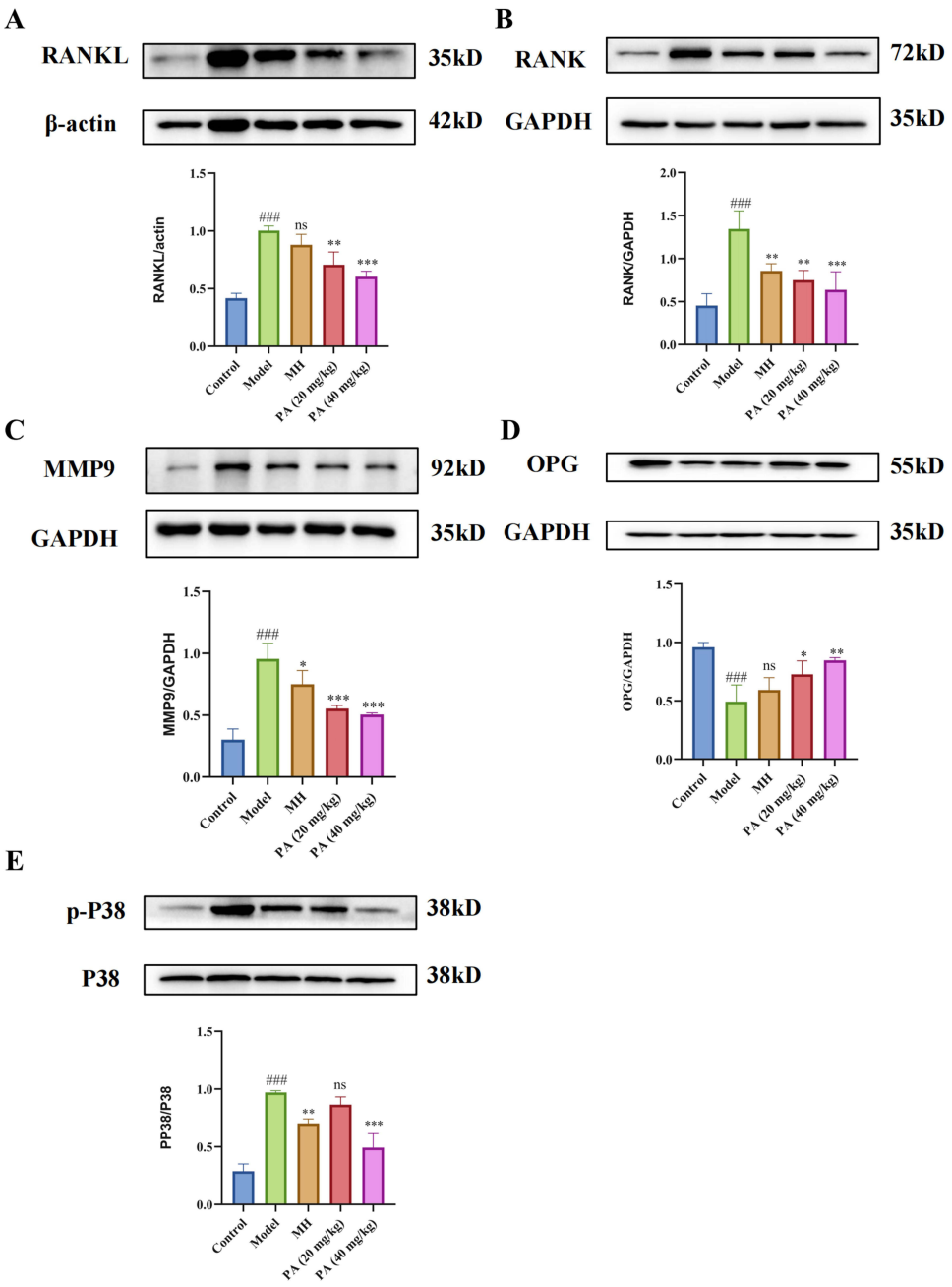

Figure 8 The amounts of (**A**) RANKL; (**B**) RANK; (**C**) OPG; (**D**) MMP-9; (**E**) p38 MAPK proteins were measured using the Western blot method (n=3). Compared with the Control, $^{\#\#\#}p < 0.001$; compared with the Model, $^{*}p < 0.05$, $^{**}p < 0.01$, $^{***}p < 0.001$; *ns*=not significant ($p > 0.05$).

positive feedback loop between IL-6 and TNF-α continuously drives MMP-9 biosynthesis, forming the molecular basis for inflammatory cascade amplification.[28]

Inflammation and alveolar bone loss are critical targets for therapeutic intervention in periodontitis. Micro-CT has become the most commonly used method for assessing alveolar bone mass and structure in animal models of periodontitis.[29] Measuring the CEJ-ABC distance (cementoenamel junction to alveolar bone crest) is a feasible approach to evaluate alveolar bone loss caused by the accumulation of periodontal pathogenic biofilms in the first molar.[30] Analysis of Micro-CT results revealed that, compared to the Model, the PA group significantly reduced the CEJ-ABC distance and the destruction at the furcation area, indicating that PA can inhibit the progression of periodontitis by reducing alveolar bone loss, which suggests that PA can curb the development of periodontitis by slowing down the

https://doi.org/10.2147/JIR.S530534

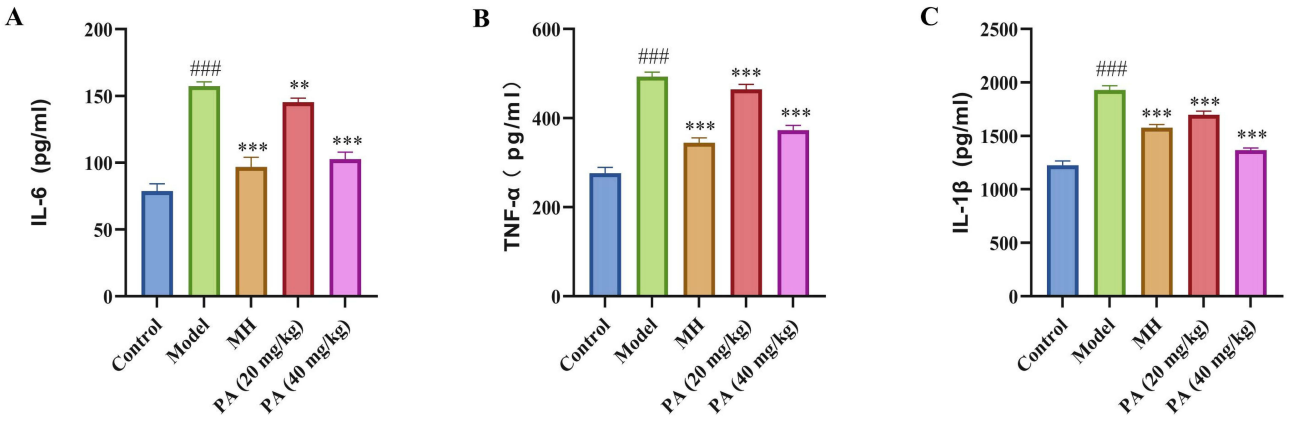

Figure 9 (A-C) ELISA was used to measure the expression levels of IL-6, TNF-α, and IL-1β in the serum of rats (n=6). (**A**) IL-6; (**B**) TNF-α; (**C**) IL-1β. Compared with the Control, $^{###}p < 0.001$; compared with the Model, $^{**}p < 0.01$, $^{***}p < 0.001$; *ns*=not significant ($p > 0.05$).

alveolar bone resorption process. Additionally, this study evaluated the effects of PA on the microarchitecture of alveolar bone in a periodontitis animal model by measuring bone microstructure parameters (Tb.Th, Tb.Sp, and BV/TV). The data demonstrated that, compared to the Model, PA intervention improved the alveolar bone loss and reduced trabecular thickness caused by periodontitis. These findings provide evidence supporting the potential utility of PA in the treatment of periodontitis.

Histological and imaging results corroborated with each other, revealing that PA significantly reduced alveolar bone loss and enhanced connective tissue attachment compared to the Model. To comprehensively analyze the potential association between inflammatory processes and ligature-induced alveolar bone damage, this study conducted a quantitative assessment, systematically scoring the levels of inflammatory cell infiltration in the periodontal tissues of each experimental group. The data demonstrated that, compared to the Model, the PA treatment group exhibited a significant reduction in inflammatory tissue scores. Furthermore, this study conducted a detailed evaluation of the local collagen fiber structure in the periodontal tissues. According to the Masson staining results, we observed severe disruption and disorganized arrangement of collagen fiber bundles in the periodontal tissues of the Model rats, whereas this damage was significantly ameliorated in the PA treatment group.

The molecular regulatory mechanism of bone metabolism revolves around the RANKL-RANK-OPG axis: When RANKL specifically binds to the RANK receptor on the membrane surface of osteoclast precursors, the bone resorption process is triggered. OPG, as a natural antagonist, maintains bone homeostasis by competitively blocking this binding.[31] In chronic inflammatory microenvironments, IL-6 exhibits destructive bidirectional regulation, both stimulating RANKL production and inhibiting OPG secretion, forming a "malignant switch" for bone destruction.[32] At the molecular level, the RANKL-RANK complex initiates NF-κB, MAPK, and other classical signaling cascades by inducing TRAF6 phosphorylation, in which TRAF6 serves as a key connector molecule (as confirmed by gene knockout models showing that its loss of function leads to osteoclast differentiation disorders and triggers osteosclerosis phenotypes).[33] NFATc1, the terminal effector of the signaling cascade, completes osteoclast differentiation by activating the expression of osteoclast-specific genes such as TRAP and CTSK. Notably, Runx2 acts as a "bidirectional regulator" of bone metabolism and it maintains bone remodeling by regulating RANKL/OPG homeostasis under physiological conditions. However, under pathological conditions (eg, tumor bone metastasis), its aberrant overexpression acts as a "molecular driver" that accelerates bone destruction through RANKL upregulation and concurrent OPG suppression.

Ligature combined with LPS-induced secretion of proinflammatory cytokines and chemokines, activating osteoclasts to accelerate bone resorption. Alveolar bone resorption represents a hallmark pathological feature of periodontitis. RANKL and RANK, primarily secreted by stromal cells and osteoblasts, serve as key regulators of osteoclastogenesis.[34] While RANKL/RANK upregulation drives osteoclast differentiation and subsequent alveolar bone loss, osteoblast-derived OPG counteracts this process by competitively binding RANKL, thereby preventing excessive bone resorption. PA treatment significantly suppressed RANKL and RANK expressions, while upregulating

OPG and Runx2 levels. As a key member of the MAPK family, p38 mediates signal transduction via phosphorylation cascades, orchestrating cellular stress responses, inflammation, and differentiation processes.[35] TRAF6-mediated activation of the p38 MAPK pathway is essential for osteoclast maturation and functional competence. RANKL-RANK binding triggers TRAF6-dependent p38 MAPK activation, subsequently phosphorylating NFATc1 to drive osteoclast differentiation. Western blot data correlated with RT-qPCR findings, confirming PA's transcriptional regulation of target genes. PA treatment concomitantly decreased protein levels of RANK, RANKL, phospho-p38, and MMP-9, along with mRNA expression of *TRAF6, NFATc1*, and *MMP-9* in periodontal tissues, while elevating OPG and Runx2 expression.

Conclusion

This study is the first to investigate the inhibitory effects of PA on periodontitis in animal experiments. A novel strategy combining network pharmacology, molecular docking, and experimental pharmacology was employed to explore the pharmacological mechanisms of PA. Network pharmacology studies revealed that MAPK8 and MAPK14 are core targets, and molecular docking was performed to investigate their interaction mechanisms. Specifically, a periodontitis model was established using the ligation method combined with LPS injection to evaluate the therapeutic effects of PA on periodontitis. In this study, the Micro-CT was used to determine alveolar bone loss, and H&E staining and Masson staining were used to examine the histological profile of alveolar bone. In addition, the ELISA was used to detect inflammation-related factors while the qRT-PCR and Western blot were used to measure p38 MAPK pathway-related indicators. The results showed that they bind well with different bonding patterns. The findings suggest that PA exerts anti-periodontitis effects by regulating the OPG/RANK/RANKL/p38 MAPK signaling pathway, indicating its potential as a treatment for periodontitis, indicating its potential as a treatment for periodontitis. This mechanistic insight provides a foundation for developing PA-based therapeutic strategies aimed at halting disease progression and preserving alveolar bone, which are critical unmet needs in periodontitis management. Furthermore, targeting this pathway with PA offers another potentially safer alternative to modulate inflammation and bone resorption.

Abbreviations

PA, Patchouli alcohol; TCMSP, trperiodontitisitional Chinese medicine; RT-qPCR, Real-Time Quantitative polymerase chain reaction; ELISA, enzyme-linked immunosorbent assay; H&E, Hematoxylin-eosin staining; IL-1β, interleukin beta 1;IL-6, interleukin-6; TNF-α, tumor necrosis factor-alpha; β-actin, Beta-actin; GAPDH, glyceraldehyde phosphate dehydrogenase; MMP-9, Matrix Metalloproteinase-9; RANK, Receptor Activator of Nuclear Factor-κB; RANKL, Receptor Activator of Nuclear Factor-κB Ligand; TRAF6, Tumor Necrosis Factor Receptor-Associated Factor 6; NFATc1, Nuclear Factor of Activated T Cells 1; p-P38, Phosphorylated p38; OPG, Osteoprotegerin; Runx2, Runt-related Transcription Factor 2.

Data Sharing Statement

All datasets are available upon reasonable request from the corresponding author. E-mail: liusijun@gzucm.edu.cn (Sijun Liu).

Institutional Review Board Statement

All animal experiments were strictly conducted in accordance with the guidelines established by the Chinese Committee for the Management of Laboratory Animals and the ethical standards for animal care and use. The study was formally approved by the Ethics Review Committee of Guangzhou University of Chinese Medicine (Approval No.: ZYD-2024-039). According to Article 32, Paragraph 1 and Paragraph 2 of the "Ethical Review Measures for Life Sciences and Medical Research Involving Human Beings" released on February 18, 2023: (1) Research conducted using legally obtained public data or data generated through observation without interfering with public behavior; (2) Research carried out using anonymized information data, may be exempted from ethical review.

Acknowledgments

Shuting Zhang and Feifei Duan are co-first authors for this study. This work was supported by the National Natural Science Foundation of China (No.82374054), Agricultural Product- Oriented Innovation Team Construction Project for Guangdong Modern Agricultural Industry Technology System (Nan-Yao Industry Technology System) (2024CXTD24).

Author Contributions

All authors made a significant contribution to the work reported, whether that is in the conception, study design, execution, acquisition of data, analysis and interpretation, or in all these areas; took part in drafting, revising or critically reviewing the article; gave final approval of the version to be published; have agreed on the journal to which the article has been submitted; and agree to be accountable for all aspects of the work.

Funding

This work was supported by the National Natural Science Foundation of China (No. 82374054), Agricultural Product-Oriented Innovation Team Construction Project for Guangdong Modern Agricultural Industry Technology System (Nan-Yao Industry Technology System) (2024CXTD24).

Disclosure

The authors declare no conflicts of interest in this work.

References

1. Hajishengallis G, Chavakis T. Local and systemic mechanisms linking periodontal disease and inflammatory comorbidities. *Nat Rev Immunol*. 2021;21(7):426–440. doi:10.1038/s41577-020-00488-6
2. Isola G, Polizzi A, Serra S, Boato M, Sculean A. Relationship between periodontitis and systemic diseases: a bibliometric and visual study. *Periodontology*. 2025. doi:10.1111/prd.12621
3. Isola G, Polizzi A, Santagati M, Alibrandi A, Iorio-Siciliano V, Ramaglia L. Effect of nonsurgical mechanical debridement with or without chlorhexidine formulations in the treatment of peri-implant mucositis. A randomized placebo-controlled clinical trial. *Clin Oral Implants Res*. 2025;36(5):566–577. doi:10.1111/clr.14405
4. Singh O, Garg T, Rath G, Goyal AK. Microbicides for the treatment of sexually transmitted HIV infections. *J Pharm*. 2014;2014:352425. doi:10.1155/2014/352425
5. Eke PI, Dye BA, Wei L, et al. Update on prevalence of periodontitis in adults in the United States: NHANES 2009 to 2012. *J Periodontol*. 2015;86(5):611–622. doi:10.1902/jop.2015.140520
6. Marconcini S, Giammarinaro E, Cosola S, Oldoini G, Genovesi A, Covani U. Effects of non-surgical periodontal treatment on reactive oxygen metabolites and glycemic control in diabetic patients with chronic periodontitis. *Antioxidants*. 2021;10(7):1056. doi:10.3390/antiox10071056
7. Nugraha AP, Ernawati DS, Narmada IB, et al. RANK-RANKL-OPG expression after gingival mesenchymal stem cell hypoxia preconditioned application in an orthodontic tooth movement animal model. *J Oral Biol Craniofac Res*. 2023;13(6):781–790. doi:10.1016/j.jobcr.2023.10.009
8. Anzai M, Watanabe-Takahashi M, Kawabata H, et al. Clustered peptide regulating the multivalent interaction between RANK and TRAF6 inhibits osteoclastogenesis by fine-tuning signals. *Commun Biol*. 2025;8(1):643. doi:10.1038/s42003-025-08047-2
9. Mo L, Zhu J, Li M, et al. Smads and AP-1 activation of TGF-β signaling upregulate transcription of osteoprotegerin in cementoblasts to inhibit osteoclastogenesis. *FASEB J*. 2024;38(22):e70171. doi:10.1096/fj.202401551R
10. de Sousa ET, de Araújo JSM, Pires AC, Lira Dos Santos EJ. Local delivery natural products to treat periodontitis: a systematic review and meta-analysis. *Clin Oral Invest*. 2021;25(7):4599–4619. doi:10.1007/s00784-021-03774-2
11. Wang Y, Sun C, Cao Y, et al. Glycyrrhizic acid and patchouli alcohol in Huoxiang Zhengqi attenuate intestinal inflammation and barrier injury via regulating endogenous corticosterone metabolism mediated by 11β-HSD1. *J Ethnopharmacol*. 2025;338(Pt 1):119025. doi:10.1016/j.jep.2024.119025
12. Wan F, Peng F, Xiong L, Chen JP, Peng C, Dai M. In vitro and in vivo antibacterial activity of patchouli alcohol from pogostemon cablin. *Chin J Integr Med*. 2021;27(2):125–130. doi:10.1007/s11655-016-2452-y
13. Xu QQ, Su ZR, Hu Z, Yang W, Xian YF, Lin ZX. Patchouli alcohol ameliorates the learning and memory impairments in an animal model of Alzheimer's disease via modulating SIRT1. *Phytomedicine*. 2022;106:154441. doi:10.1016/j.phymed.2022.154441
14. Kawasaki M, Kuwano K, Hagimoto N, et al. Protection from lethal apoptosis in lipopolysaccharide-induced acute lung injury in mice by a caspase inhibitor. *Am J Pathol*. 2000;157(2):597–603. doi:10.1016/s0002-9440(10)64570-1
15. Wu YH, Kuraji R, Taya Y, Ito H, Numabe Y. Effects of theaflavins on tissue inflammation and bone resorption on experimental periodontitis in rats. *J Periodontal Res*. 2018;53(6):1009–1019. doi:10.1111/jre.12600
16. Wang X, Wang W, Li W, et al. Evaluation of the efficacy of Hylotelephium purpureum gel in the treatment of experimental periodontitis. *Biomed Rep*. 2018;8(4):378–384. doi:10.3892/br.2018.1065
17. Golub LM, Lee HM. Periodontal therapeutics: current host-modulation agents and future directions. *Periodontol 2000*. 2020;82(1):186–204. doi:10.1111/prd.12315
18. Tibúrcio-Machado CS, Michelon C, Zanatta FB, Gomes MS, Marin JA, Bier CA. The global prevalence of apical periodontitis: a systematic review and meta-analysis. *Int Endodontic J*. 2021;54(5):712–735. doi:10.1111/iej.13467

19. Herath TD, Darveau RP, Seneviratne CJ, Wang CY, Wang Y, Jin L. Tetra- and penta-acylated lipid A structures of Porphyromonas gingivalis LPS differentially activate TLR4-mediated NF-κB signal transduction cascade and immuno-inflammatory response in human gingival fibroblasts. *PLoS One*. 2013;8(3):e58496. doi:10.1371/journal.pone.0058496
20. Wang Z, Zeng H, Wang C, et al. Tim4 deficiency reduces CD301b(+) macrophage and aggravates periodontitis bone loss. *Int J Oral Sci*. 2024;16(1):20. doi:10.1038/s41368-023-00270-z
21. Chen X, Dou J, Fu Z, et al. Macrophage M1 polarization mediated via the IL-6/STAT3 pathway contributes to apical periodontitis induced by Porphyromonas gingivalis. *J Appl Oral Sci*. 2022;30:e20220316. doi:10.1590/1678-7757-2022-0316
22. Cui D, Lyu J, Li H, et al. Human β-defensin 3 inhibits periodontitis development by suppressing inflammatory responses in macrophages. *Mol Immunol*. 2017;91:65–74. doi:10.1016/j.molimm.2017.08.012
23. Kanzaki H, Makihira S, Suzuki M, et al. Soluble RANKL cleaved from activated lymphocytes by TNF-α-converting enzyme contributes to osteoclastogenesis in periodontitis. *J Immunol*. 2016;197(10):3871–3883. doi:10.4049/jimmunol.1601114
24. Pathak JL, Fang Y, Chen Y, et al. Downregulation of macrophage-specific Act-1 intensifies periodontitis and alveolar bone loss possibly via TNF/NF-κB Signaling. *Front Cell Develop Biol*. 2021;9:628139. doi:10.3389/fcell.2021.628139
25. Franco C, Patricia HR, Timo S, Claudia B, Marcela H. Matrix metalloproteinases as regulators of periodontal inflammation. *Int J Mol Sci*. 2017;18(2):440. doi:10.3390/ijms18020440
26. Luchian I, Goriuc A, Sandu D, Covasa M. The role of matrix metalloproteinases (MMP-8, MMP-9, MMP-13) in periodontal and peri-implant pathological processes. *Int J Mol Sci*. 2022;23(3):1806. doi:10.3390/ijms23031806
27. Checchi V, Maravic T, Bellini P, et al. The role of matrix metalloproteinases in periodontal disease. *Int J Environ Res Public Health*. 2020;17(14):4923. doi:10.3390/ijerph17144923
28. Zhang H, Liu L, Jiang C, Pan K, Deng J, Wan C. MMP9 protects against LPS-induced inflammation in osteoblasts. *Innate Immun*. 2020;26(4):259–269. doi:10.1177/1753425919887236
29. Chavez MB, Kolli TN, Tan MH, et al. Loss of discoidin domain receptor 1 predisposes mice to periodontal breakdown. *J Dent Res*. 2019;98(13):1521–1531. doi:10.1177/0022034519881136
30. Kang S, Liu S, Dong X, et al. USP4 depletion-driven RAB7A ubiquitylation impairs autophagosome-lysosome fusion and aggravates periodontitis. *Autophagy*. 2025;21(4):771–788. doi:10.1080/15548627.2024.2429371
31. Liu W, Zhang X. Receptor activator of nuclear factor-κB ligand (RANKL)/RANK/osteoprotegerin system in bone and other tissues (review). *Mol Med Rep*. 2015;11(5):3212–3218. doi:10.3892/mmr.2015.3152
32. Mori T, Miyamoto T, Yoshida H, et al. IL-1β and TNFα-initiated IL-6-STAT3 pathway is critical in mediating inflammatory cytokines and RANKL expression in inflammatory arthritis. *Int Immunol*. 2011;23(11):701–712. doi:10.1093/intimm/dxr077
33. Du Y, Chen H, Zhou L, et al. REGγ is essential to maintain bone homeostasis by degrading TRAF6, preventing osteoporosis. *Proc Natl Acad Sci USA*. 2024;121(47):e2405265121. doi:10.1073/pnas.2405265121
34. Leibbrandt A, Penninger JM. RANK/RANKL: regulators of immune responses and bone physiology. *Ann NY Acad Sci*. 2008;1143(1):123–150. doi:10.1196/annals.1443.016
35. Su H, Liu L, Yan Z, et al. Therapeutic potential of total flavonoids of Rhizoma Drynariae: inhibiting adipogenesis and promoting osteogenesis via MAPK/HIF-1α pathway in primary osteoporosis. *J Orthopaedic Surg Res*. 2025;20(1):260. doi:10.1186/s13018-025-05665-8